

RELATIVISTIC SPIN-PRECESSION IN BINARY PULSARS

MICHAEL KRAMER*

Max-Planck-Institut für Radioastronomie

Auf dem Hügel 69

53121 Bonn, Germany

and Jodrell Bank Centre for Astrophysics, University of Manchester

Turing Building, Oxford Road

Manchester M13 9PL, UK

**E-mail: mkramer@mpi-fr.de*

After the first prediction to expect geodetic precession in binary pulsars in 1974, made immediately after the discovery of a pulsar with a companion, the effects of relativistic spin precession have now been detected in all binary systems where the magnitude of the precession rate is expected to be sufficiently high. Moreover, the first quantitative test leads to the only available constraints for spin-orbit coupling of a strongly self-gravitating body for general relativity (GR) and alternative theories of gravity. The current results are consistent with the predictions of GR, proving the effacement principle of spinning bodies. Beyond tests of theories of gravity, relativistic spin precession has also become a useful tool to perform beam tomography of the pulsar emission beam, allowing to infer the unknown beam structure, and to probe the physics of the core collapse of massive stars.

Keywords: neutron stars; pulsars; experimental tests of theories of gravity; general relativity; supernovae; radio emission

1. Introduction

The theory of general relativity predicts, as other alternative relativistic theories of gravity, that space-time is curved by the presence of matter. It is this curvature that then describes how matter is moving. A direct way to verify this concept of curved space-time is to measure, for instance, a deflection of light¹ or a “Shapiro-delay”,² i.e. an extra flight-time of an electromagnetic signal when it passes near a mass and transverses its curved space-time compared to the flight-time in flat space-time away from masses (e.g. Ref. 3). Another way of measuring the impact of curved space-time is the usage of a gyroscope orbiting a central mass. This effect, known as geodetic precession or de Sitter precession represents the effect on a vector carried along with an orbiting body such that the vector points in a different direction from its starting point (relative to a distant observer) after a full orbit around the central object.^{4,5} Experimental verification has been achieved by precision tests in the solar system, e.g. by Lunar Laser Ranging (LLR) measurements, or recently by measurements with the Gravity Probe-B satellite mission (see Ref. 1 for a review of experimental tests). However, these tests are done in the weak field conditions of the solar systems, while it is important to also perform tests in the strong-field regime. What is therefore needed are compact, spinning test masses where we can infer and monitor the orientation of the spin direction when they are in motion about a binary orbit. Fortunately, nature provides us with such ideal labs: binary radio pulsars.

In binary system one can interpret the observations, depending on the reference frame, as a mixture of different contributions to relativistic spin-orbit interaction. One contribution comes from the motion of the first body around the centre of mass of the system (deSitter-Fokker precession), while the other comes from the dragging of the internal frame at the first body due to the translational motion of the companion.⁶ Hence, even though we loosely talk about geodetic precession, the result of the spin-orbit coupling for binary pulsar is more general, and hence we will call it *relativistic spin-precession*.

The consequence of relativistic spin-precession is a precession of the pulsar spin about the total angular momentum vector, changing the orientation of the pulsar relative to Earth. This allows us to detect this effect, to study its impact on the observed pulsar emission, to gain information about the pulsar itself and, last but not least, to test the predictions for relativistic spin-orbit coupling in general relativity and alternative theories of gravity.

This contribution will briefly review the basic properties of pulsars that are needed to understand and interpret the seen effects in pulsars, before it presents a summary of those observations where relativistic spin-orbit coupling has been detected and studied. Finally, I will summarize the applications of this effect in fields ranging from core collapse physics in massive stars to testing theories of gravity.

2. Pulsars

Pulsars are rotating neutron stars that emit a radio beam that is eventually powered by the pulsars' rotational energy and that is centred on the magnetic axis of the neutron star. As the magnetic axis and the hence the beam are inclined to the rotation axis, the pulsar acts as a cosmic lighthouse, and a pulsar appears as a pulsating radio source. The moment of inertia and the stored rotational energy of pulsars are large, so that in particular the fast rotating millisecond pulsars deliver a radio "tick" per rotation with a precision that rivals the best atomic clocks on Earth. Corresponding pulse (or spin) periods range from 1.4 ms to 8.5 s. As they concentrate an average of 1.4 solar masses on a diameter of only about 20 km, pulsars are exceedingly dense and compact, representing the densest matter in the observable universe. The resulting gravitational field near the surface is large, enabling strong-field tests of gravity. Here we describe a cosmic experiment where we see these spinning tops orbiting another massive companion. In order to infer and monitor their spin precession, we do not utilize the accurate time-of-arrival measurements of their pulses as done in most other pulsar timing experiments, but we study the pulsar radio emission.

2.1. Pulsar radio emission

After more than 40 years of pulsar research, the details of the actual emission process still elude us, but our basic understanding is sufficient to perform the experiments described later. In our straw-man model, the high magnetic field of the rotating

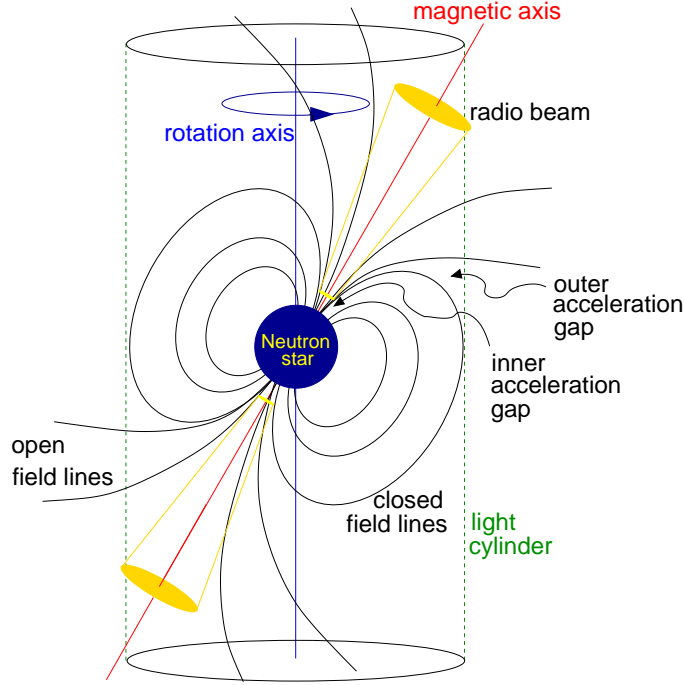


Fig. 1. Basic model of a radio pulsar. Taken from Ref. 7.

neutron star ($B_{\text{surf}} \sim 10^8 - 10^{14}$ Gauss) induces a huge electric quadrupole field and an electromagnetic force that exceeds gravity by ten to twelve orders of magnitudes. Charges are pulled out easily from the surface, and the result is a dense, magnetized plasma that surrounds the pulsar. The strong magnetic field forces the plasma to co-rotate with the pulsar like a rigid body. This co-rotating *magnetosphere* can only extend up to a distance where the co-rotation velocity reaches the speed of light^a. This distance defines the so-called light cylinder which separates the magnetic field lines into two distinct groups, i.e. *open and closed field lines*. Closed field lines are those which close within the light cylinder, while open field lines would close outside. The plasma on the closed field lines is trapped and will co-rotate with the pulsar forever. In contrast, plasma on the open field lines can reach highly relativistic velocities and can leave the magnetosphere, creating the observed radio beam at a distance of a few tens to hundreds of km above the pulsar surface (see Fig. 1).

^aStrictly speaking, the Alfvén velocity will determine the co-rotational properties of the magnetosphere.

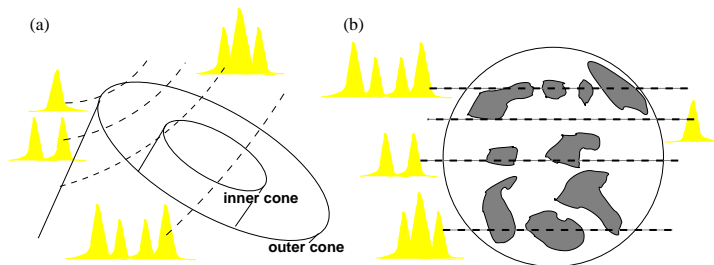


Fig. 2. Creation of multi-component pulse profiles in two possible beam models. (a) A nested cone structure, (b) a patchy beam structure. See text for details. Taken from Ref. 7.

2.1.1. The structure of the pulsar beam

The radio beams show high time-variability in individual recorded pulses that reflects the instantaneous plasma processes in the pulsar magnetosphere at the moment when the beam is directed towards Earth. Despite this variety displayed by the single pulses, the mean pulse shape computed by averaging a few hundred to few thousand of pulses is usually very stable.⁷ In contrast to the snapshot provided by the individual pulses, the average pulse shape, or *pulse profile*, can be considered as a long-exposure picture, revealing the global circumstances in the magnetosphere. These are mostly determined by geometrical factors and the strong magnetic field. Apart from a distinct evolution with radio frequency, the same profiles are obtained, no matter where and when the pulses used to compute the average have been observed. Changes in the pulse profile therefore usually reflect a change in the pulsar geometry that can be detected and monitored.^b

The observed pulse profiles show a large variety of shapes. Although each pulsar exhibits a slightly different profile – almost like a unique fingerprint – a systematic pattern can be recognized. The most simple model successfully describing the beam shapes is that of a hollow cone of emission.⁸ It is based on the idea that the outermost open field lines, which show the largest curvature among the “emitting field lines”, should be associated with the strongest emission, leading naturally to a cone-like structure. Observations show that this picture is vastly oversimplified, since we also often observe components inside this hollow-cone structure. Those inner component may be positioned in preferred located (e.g. in the cone centre as a “core” component⁹ and/or in a nested cone structure¹⁰) or in a seemingly random pattern of a patchy beam shape¹¹ (see Fig. 2). It is clear, however, that the observed pulse profile depends eventually on how our line-of-sight cuts the emission cone. With relativistic spin precession changing our path through the beam, we therefore not only expect the observed pulse shape to change, but we also have the

^b For completeness we note that Lyne et al. have found evidence for long-term changes in the pulse profile which are correlated with changes in the pulse-spin down.

chance to actually probe the beam structure in latitudinal direction to test specific emission theories (see Section 4.3).

2.1.2. Polarisation — Signatures of Geometry

An important and most useful property of pulsar radio emission is its typical high degree of polarisation. The radiation is often 100% elliptically polarized, and it is usual practice to separate the polarisation into linearly and circularly polarized components. The linear component is often the far dominating one, although pulsars with circular components as strong as 30% or more are not uncommon. Polarisation serves as a useful diagnostic tool to obtain information about the viewing geometry.¹²

The strong coupling of the outwards-moving plasma to the magnetic field lines in the pulsar magnetosphere has the effect that the plane of polarisation of the linear component is determined by the plane embedding the corresponding field line. The observed position angle (PA) of the linear polarisation is then given by the projection of this direction onto our line-of-sight. The result is an S-like curve of the PA whose shape depends on the angle between the rotation and magnetic axes, α , as well as on the distance of our line-of-sight to the magnetic pole, β (see inset in Fig. 4). If our line-of-sight cuts the emission beam close to the magnetic axis, the PA changes rapidly when crossing the centre of the beam. If the impact angle β is large and we are cutting the cone further away from the pole, the transition is much smoother and the PA swing much flatter.⁷

By measuring the polarisation characteristics of a pulsar, we can in principle win information about the pulsar's orientation towards us. In practice, fitting this *rotating vector model*¹³ (RVM) turns out to be often difficult. Although the majority of observed PA swings can be well described by the RVM after correcting for sometimes occurring orthogonal modes (i.e. jumps of the PA by nearly 90° which are probably magnetospheric propagation effects), the uncertainties in the obtained angles representing the geometry are typically large. The reason is not a failure of the model, but simply the small size of beam of most pulsars, which provides constraints to the fit for only the small fraction of the pulse period when the pulse is actually observed, which is typically only 4% (see Ref. 7 for more details).

Observations of normal (i.e. non-recycled pulsars, see below for the evolutionary differences) pulsars confirm the geometrical meaning of the RVM.¹² This is less clear for recycled pulsars (e.g. Ref. 14), but detecting a change in the observed PA swing curve will immediately indicate a change in viewing geometry. Another way to detect changes in the viewing geometry was pointed out recently by Kramer & Wex (2009, Ref. 15) who presented a method to use the absolute position angle measurement (i.e. a PA measurement tied to a celestial reference frame) to determine a change in the spin direction of pulsars. This method has now been successfully applied to PSRs J1141–6545 and J1906+0746 (see Fig. 4) as described later.

2.1.3. *Formation & Evolution*

Relativistic spin precession in binary pulsars only occurs if the pulsar spin vector is misaligned with the total angular momentum vector. If precession is observed, observations can be used to determine this misalignment angle. The question as to whether the spin vector is aligned or not depends on the evolutionary history of the pulsar and the binary system as a whole.

Neutron stars and pulsars are born in a supernova explosions, conventionally believed to be the core collapse of a massive star although alternative routes seem to exist (see Section 4.2). Most pulsars loose a possible companion in this supernova explosion but those which retain it may be spun-up in a later period of their life. Those pulsars appear as millisecond (or recycled) pulsars with short spin period and are expected to be still in orbit with the remnant of the companion star.

The mass of the companion star determines the duration of the accretion process and the fate of the system. If the companion is of low mass, it evolves slowly and the mass transfer can be sufficiently long to spin up the pulsar to periods of a few milliseconds or less. The end product would be a pulsar - white dwarf system where due to the exchange of angular momentum and tidal interactions all spin vectors are expected to be aligned, so that no spin-precession should occur.

If the companion star is massive enough to undergo a supernova explosion on its own, the evolution timescale is shorter and the accretion process is cut short. The result for the pulsar is a spin period of tens of millisecond and a neutron star companion, should the system survive this second supernova explosion. The formation of the second-born neutron star is likely to occur in an *asymmetric supernova explosion* which imparts a kick on the companion that tilts the new orbit relative to the pre-supernova configuration. The spin vector of the recycled pulsar is unaffected and now misaligned with the new total angular momentum vector – relativistic spin precession should occur. Variations to the latter statement are possible if the second supernova was “gentle” and produced only a low-velocity kick to the second neutron star. In this case, as it seems to be observed in the Double Pulsar (see below), the orbital plane direction is hardly changed and the recycled pulsar may not precess notably.

Under certain conditions, it is possible that we see radio emission of the young, second-born pulsar in a binary system. This seems to be the case in J1141–6545, J1906+0646 and, of course, in the Double Pulsar. Here, we have no constraints on the possible direction of the pulsar spin vector as this is determined by the individual properties of the corresponding supernova explosion. It is therefore highly likely that spin vectors are misaligned, so that spin precession is expected to be observed.

3. The experiments

Since the orbital angular momentum is much larger than the angular momentum of the pulsar, the orbital spin practically represents a fixed direction in space, defined by the orbital plane of the binary system. Therefore, if the spin vector of the pulsar

is misaligned with the orbital spin, relativistic spin-precession leads to a change in viewing geometry, as the pulsar spin precesses about the total angular momentum vector. Consequently, as many of the observed pulsar properties are determined by the relative orientation of the pulsar axes towards the distant observer on Earth, we should expect a modulation in the measured pulse profile properties, namely its shape and polarisation characteristics. This was immediately recognized in the ground-breaking work by Damour & Ruffini (Ref. 16). Shortly after the discovery of the first binary pulsar by Hulse & Taylor in 1974 – and even before its publication¹⁷ – Damour & Ruffini pointed out that such a modulation should occur with a periodicity of that of the precession period.

The precession rate as predicted by general relativity (GR) is given by^{6,18}

$$\Omega_p = T_\odot^{2/3} \times \left(\frac{2\pi}{P_b} \right)^{5/3} \times \frac{m_c(4m_p + 3m_c)}{2(m_p + m_c)^{4/3}} \times \frac{1}{1 - e^2} \quad (1)$$

where P_b is the period and e the eccentricity of the orbit. We express the masses m_p and m_c in units of solar masses (M_\odot) and define the constant $T_\odot = GM_\odot/c^3 = 4.925490947\mu s$. G denotes the Newtonian constant of gravity and c the speed of light. It is useful to note that, in GR, for equal masses

$$\Omega_p = \frac{7}{24} \dot{\omega} \sim 0.3 \dot{\omega}. \quad (2)$$

Spin precession may have a direct effect on the timing, as it causes the polar angles of the spin and, hence, the aberration parameters of the timing model to change with time (see Refs. 7,19 for details). However, the consequences for the observed emission properties are, usually, much more apparent and easier to identify as changes in the timing parameters may get absorbed into other parameters for a limited observing span.

Due to the changing cuts through the emission beam as the pulsar spin axis precesses, we firstly expect the profile to narrow or widen depending on the precession phase and beam structure. As this also changes the distance of the observer's line-of-sight to the magnetic axis, the position angle swing should become flatter or steeper, depending on whether the impact angle β is decreasing or increasing, respectively. In comparison to the observed total power profile, we can also expect the polarisation properties to be more sensitive to the local conditions in the magnetosphere that are probed by our line-of-sight, suggesting that changes in polarised emission go further than just changing the position angle slope.

In order to see a measurable effect in any binary pulsar, *a)* the spin axis of the pulsar needs to be misaligned with the total angular momentum vector and *b)* the precession rate must be sufficiently large compared to the available observing time to detect a change in the emission properties. Table 1 lists the known Double Neutron Star Systems (DNS) which typically show the largest degree of relativistic effects due to the often short eccentric binary orbits. However, the last entry in the table is PSR J1141–6545 which is a relativistic system with a white dwarf companion.²⁰

Those pulsars that are marked with an asterisk have been identified as pulsars showing relativistic spin precession. We will discuss them in detail later below. What is apparent by inspecting the precession rate as computed by Eqn. (1) is that the top 5 out of 8 sources with a value for the expected precession rate indeed show the effect. The only exceptions are pulsar A in the Double Pulsar (i.e. PSR J0737–3039) and PSRs J1756–2251 and J1829+2456. We understand the lack in pulsar A by a possible alignment of its spin axis with the orbital spin for which we have independent evidence that will be discussed in Sec. 4.2. PSR J1756–2251 is a relatively new discovery²¹ with a rather simple profile, so that a detection has not been made yet. The expected detection rate for J1828+2456 is very likely too small to lead to significant observable effects. In contrast, PSR B1534+12 has a relatively small precession rate of 0.5 deg yr^{-1} but as the second DNS discovered it is well studied with a long history of excellent polarisation data.²² Indeed, a third criterion *c)* that has been usually important for actually making a firm detection of spin precession is the usage or availability of long-term observations with identical or similar instrumental set-up. Nowadays, as coherent de-dispersion systems with many-bit digitization deliver nearly identical results, observations made at different telescopes or with different data acquisition systems can be combined much easier.

Table 1. DNSs sorted according to the expected relativistic spin precession rate. Also included is PSR J1141–6545 which is in a relativistic orbit about a white dwarf companion. Pulsars marked with an asterisk have been identified of showing spin precession. For sources where no precession rate is listed, the companion mass could not be accurately measured yet, indicating however, that the precession rate is low.

PSR	$P(\text{ms})$	$P_b \text{ (d)}$	$x(\text{lt-s})$	e	$\Omega_p \text{ (deg yr}^{-1}\text{)}$
J0737–3039A/B*	22.7/2770	0.10	1.42/1.51	0.09	4.8/5.1
J1906+0746*	144.1	0.17	1.42	0.09	2.2
B2127+11C*	30.5	0.34	2.52	0.68	1.9
B1913+16*	59.0	0.33	2.34	0.62	1.2
J1756–2251	28.5	0.32	2.76	0.18	0.8
B1534+12*	37.9	0.42	3.73	0.27	0.5
J1829+2456	41.0	1.18	7.24	0.14	0.08
J1518+4904	40.9	8.64	20.0	0.25	–
J1753–2240	95.1	13.63	18.1	0.30	–
J1811–1736	104.2	18.8	34.8	0.83	–
J1141–6545*	394.0	0.20	1.89	0.17	1.4

3.1. PSR B1913+16 – The Hulse-Taylor Pulsar

The first binary pulsars discovered¹⁷ was also the first DNS to be found, and the system remained the most relativistic one known until the discovery of the Double Pulsar (see Sec. 3.5). With its discovery it was immediately recognized that it would be a superb laboratory for relativistic gravity.¹⁷ In particular the possible detection of spin precession was pointed out from the start.¹⁶ The system parameters in

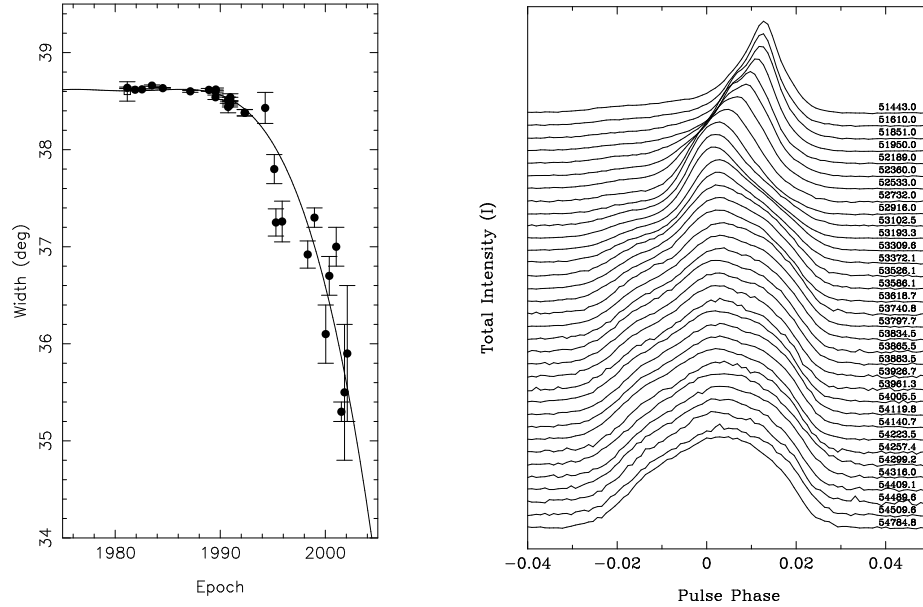


Fig. 3. Pulse changes caused by relativistic spin precession. Left) Observed component separation for PSR B1913+16 (Kramer, priv. comm.), Right) measured pulse profiles for PSR J1141–6545.²⁵ The right hand scale gives the observing date in Modified Julian Day, spanning from Sep 22, 1999, at the top to Nov 11, 2008, at the bottom.

Table 1 infer a precession rate that is relatively high, indeed promising to detect the effect on a reasonable time scale. Weisberg et al. (1989, Ref. 23) showed clearly that in about 10 years of observations, the two prominent peaks in the pulse profile had changed their relative amplitude significantly by about 1.2% per year. While this change was attributed to the effects of spin precession, this study did not detect the expected change in pulse width, unfortunately. A polarisation study²⁴ was also inconclusive as that changes in the polarisation properties that could be attributed to spin precession were not found. The authors pointed out that the beam pattern could be patchy or that the presence of a “core” beam component could disturb the regular S-like like position angle swing that one would expect to see changing.

In 1998, using data from the Effelsberg telescope, combined with the original Arecibo observations by Taylor, Weisberg and co-workers, it was possible to show that the change in relative amplitude was continuing with a rate found by Weisberg et al.²⁶ Moreover, for the first time a narrowing of the pulse profile was detected, in accordance with a simple cone-like beam model (see Fig. 3). Fitting such a model to the observed profile width data, the full geometry of the system could be determined, resulting in a measurement of the angle between the pulsar spin and the total angular momentum vector, which is an imprint of the asymmetric supernova explosion forming this system (see Section 4.2). The fit to the data also

predicts that the pulsar will disappear by moving out of our line-of-sight around the year 2025. These results were later confirmed by Weisberg & Taylor (Refs. 27,28) using new high quality Arecibo data. They also used the measured profile to perform a study of the 2-dimensional beam pattern of a pulsar for the first time – a technique that we will refer to as “beam tomography” (see Section 4.3).

3.2. *PSR B1534+12*

The second discovered DNS, PSR B1534+12, has an orbital period of 10 h and an eccentricity of 0.27. The determined masses result in a precession rate of 0.5 deg per year, suggesting that the effects of relativistic spin precession would be measurable. Indeed, this source was the first one to reveal the predicted changes in polarisation characteristics, aided by the existence of a highly polarized interpulse component that enabled a precise RVM fit and the determination of the impact parameter β and its change with time.^{22,29,30} Moreover, in addition to the secular profile changes due to spin precession, the effect of orbital aberration, causing the cut through the emission beam to change with orbital phase, was also detected for the first time,²² providing direct evidence that pulsars are indeed *rotating* neutron stars. A combination of these results led to the first independent limits on the precession rate that, albeit with low precision, was consistent with the predicted GR value.

3.3. *PSR J1141–6545*

The binary pulsar J1141–6545 is a remarkable system as it harbours a young 394-ms pulsar in a relativistic eccentric 4.5-h orbit about a massive white dwarf companion.^{20,31} We therefore observe a non-recycled pulsar, formed in a recent SN explosion that almost certainly left a pulsar with a spin-axis that is misaligned with the orbital momentum vector. With an expected precession rate of 1.4 deg per year, the pulsar was immediately suggested to be a prime candidate for spin-precession studies. In fact, spin-precession was put forward to explain why the rather strong radio source visible as the young pulsar had not been detected in a previous low-frequency survey for pulsars, covering the source position in July 1993.³¹ Unfortunately, like in a cosmic conspiracy, the data for this particular pointing have been lost, so that this hypothesis cannot be tested anymore against possible effects of radio interference which may have masked the pulsar.

The pulsar was monitored independently by two groups, i.e. our group around the initial discovery team and the Swinburne group who were the first to publish the profile variations³² which are clearly and easily visible both in total power and polarisation. Figure 3 presents the results of our monitoring project that demonstrate that the assumption of a cone-like beam structure, invoked successfully for modeling PSR B1913+16 (see Sec. 3.1), is much too simple for this source. The only way of obtaining information from the observed relativistic spin precession for geometry determination, beam tomography or even GR tests, is therefore given by

the attempt to understand the changing polarisation behaviour of this rather highly polarised source.

The available data indeed offer an opportunity to apply a new method for studies of relativistic spin precession that was not possible before. It was noted by Kramer & Wex (Ref. 15) that due to the precession of the spin vector and hence its changing projection on the sky, the absolute polarisation angle (PA), reflecting this direction, should also show a periodic variation with time (cf. Ref. 7). For the well-calibrated Parkes data, this absolute position angle information was available for a sufficiently long time to apply this method for the first time. Our results published in Ref. 25 indeed show the expected PA variation that can be modelled by the formalism introduced in Ref. 15. Using a global fit of all available PA data measured at carefully selected pulse longitudes a self-consistent description of the geometry and precession parameters is achieved. In a least-squares fit of only 4 free model parameters (i.e. misalignment angle, precession phase, absolute PA offset and magnetic inclination angle) to 920 data points covering 5 years of observations, we achieve a reduced $\chi^2 = 7.4$. We find that the spin-orbit misalignment angle is about 110 deg. At the start of our observations, the impact parameter β was about 4 deg in magnitude and it reached a minimum very close to the magnetic pole around early 2007, consistent with the observed pulse width variations. We have therefore mapped approximately one half of the emission beam, which we further discuss in Sec. 4.3.

PSR J1141–6545 was not detected in the Parkes 70cm survey³³ although, even at the present relatively low flux-density levels, a detection with signal/noise ratio of the order of 50 would have been expected. Observations within half a beamwidth of the pulsar position were made 1993 July 14 (MJD 49182). According to the fitted geometry model, β at that time was about 8 deg. This non-detection therefore suggests that the beam half-width in latitude is ~ 8 deg, although this must be qualified because of the patchy beam structure. Observations over the next decade or two will establish whether or not this is the case for PSR J1141–6545 as β returns to large (negative) values. Indeed, with the reversal in the rate of change of the impact parameter, we predict that over the next decade we will see a reversed “replay” of the variations observed in the past decade, providing an excellent test for the made modelling. While we will also learn a big deal about the beam structure, given the fact that the beam does not seem to follow an organized pattern, it is unlikely that we can use our observations for a quantitative test of GR.

3.4. *PSR J1906+0746*

This peculiar system shares similarities with the previous system J1141–6545 in that we see the precession of a young, unrecycled neutron star. In contrast, however, the companion is most likely another neutron star.³⁴ Due to the young age and its 144-ms period, the timing precision for J1906+0746 is unfortunately limited. However, the orbit is eccentric, $e = 0.09$, and rather short, $P_b = 4.1$ h, so that relativistic effects are seen. The measurement of an periastron advance and an “Einstein

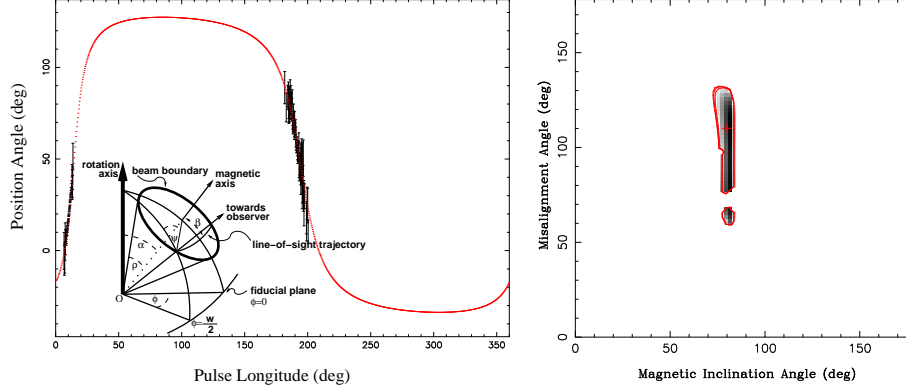


Fig. 4. Left) Polarisation angle swing measured for PSR J1906+0746. Fitting a simple geometrical “rotating vector model” as shown in the inset, the solid line is derived. Right) Applying the Kramer & Wex model, the magnetic inclination angle α and the misalignment angle between pulsar spin and orbital momentum vector can be constrained (Desvignes et al., in prep).

delay” (i.e. the combined effect of gravitational redshift and a second-order Doppler effect) imply neutron star masses of $1.35M_{\odot}$ and $1.26M_{\odot}$, respectively, resulting in a GR precession rate of 2.16 deg yr^{-1} . This large precession rate (i.e. twice as large as for the Hulse-Taylor pulsar and half the size as for the Double Pulsar) manifests itself easily in the observed pulse profile which (now) exhibits a strong interpulse separated from the main pulse by half a period. The first indication that spin precession is occurring in this system was indeed noticed when the discovery observation in 2005 was compared with a serendipitous observations from 1998 where the interpulse was missing.³⁴ In following monitoring observations it became also clear that the separation of the interpulse and main pulse is slowly decreasing with time,^{35–37} indicating a steady change in geometry. Fortunately, both main and interpulse of PSR J1906+0746 are also highly polarised, so that the RVM fit is very well constrained due to the wide range of available pulse longitudes during the fit (see Fig. 4). This allows two ways of measuring the change in geometry: Firstly, one can fit a RVM separate to data of each epoch where the uncertainty in derived angles is sufficiently small to detect a systematic change in the impact angle. Secondly, one can apply the model by Kramer & Wex (Ref. 15) and fit all epochs simultaneously with only four parameters. With a reduced $\chi^2 = 1.21$ and 632 degrees of freedom, the least-squares fit is extremely good, confirming the suspected orthogonal geometry of the pulsar and a very large misalignment angle between 60 and 120 deg (see Fig. 4). The possibility to obtain a precise RVM fit using absolutely calibrated polarisation data promises a quantitative test of relativistic spin precession in the future.

3.5. PSR J0737–3039 – *The Double Pulsar*

In 2003 a binary system was discovered where at first one member was identified as a mildly recycled pulsar with a 23 ms period³⁸ before then the companion was also recognized as a young radio pulsar with a period of 2.8 s.³⁹ Both pulsars, now known as PSR J0737–3039A and PSR J0737–3039B, respectively, (or “A” and “B” hereafter), orbit each other in less than 2.5 hours in a slightly eccentric orbit. As a result, the system is not only the first and only double neutron star system where both neutron stars are visible as active radio pulsars, but it is also the most relativistic binary pulsar known to date.

As the most relativistic binary system known to date, we expect a large amount of spin precession in the Double Pulsar system. Indeed, as shown in Tab. 1, the precession periods should be 75 years for A and 71 years for B. Despite careful studies, profile changes for A have not been detected, suggesting that A’s misalignment angle is rather small.^{40–42} In contrast, changes in the light curve and pulse shape on secular timescales⁴³ reveal that this is not the case for B. In fact, B had been becoming progressively weaker and disappeared from our view in 2009.⁴⁴ Making the valid assumption that this disappearance is solely caused by relativistic spin precession, it will only be out of sight temporarily until it reappears later. Modeling suggests that, depending on the beam shape, this will occur in about 2035 but an earlier time cannot be excluded. The geometry that is derived from this modeling is consistent with the results from complementary observations of spin precession, visible via a rather unexpected effect described in the following.

The orbit of the Double Pulsar is seen nearly edge on, i.e. the inclination angle of the orbit is measured (using a Shapiro delay) to be 88 deg.³ This leads to ~ 30 -s long eclipses of A that are caused by the blocking rotating magnetosphere of B at superior conjunction. Applying a simple successful geometrical model, Breton et al. (Ref. 45) were able to explain the regular bursts of emission of A seen during the dark eclipse phases, which are separated by a full- or half-period of B. As this pattern is determined by the three-dimensional orientation of the magnetosphere of B, which is centred on the precessing pulsar spin, changes in the eclipse pattern with time were expected and found: eclipse monitoring over the course of several years shows exactly the expected changes, with model fitting indicating a constant magnetic inclination angle and constant misalignment angle, but an azimuthal spin position changing with a rate of $\Omega_{p,B} = 4.77^{+0.66}_{-0.65}$ deg yr^{−1}. As shown in Tab. 1, this value is fully consistent with the value expected GR. This measurement, however, also allows to tests alternative theories of gravity and their prediction for relativistic spin-precession in strongly self-gravitating bodies for the first time (see Section 4.1).

4. Applications

As demonstrated, relativistic spin precession is now observed in a variety of sources and has become by now a tool with applications that go beyond simply detecting the effect as a further phenomenon predicted by GR. Firstly, however, we discuss

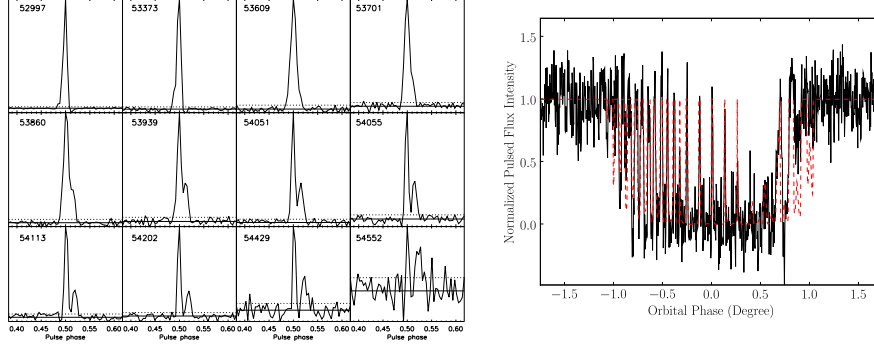


Fig. 5. Left) Pulse profiles of B in the Double Pulsar at 12 different days demonstrating the disappearance of the pulsar.⁴⁴ Right) Observed eclipse of pulsar A caused by the magnetosphere of B. The distinctive pattern depends on B's orientation and changes as a function of time.⁴⁵

exactly this usage of spin-precession.

4.1. Testing theories of gravity

The phenomena observed in the pulse structure of relativistic pulsars is consistent with the predictions of relativistic spin precession. For a real test of GR or other alternative theories of gravity a quantitative measurement of spin precession parameters are however needed. The simplest approach is to measure the rate of precession, Ω_p , and to compare it with the expected values (Tab. 1). Usually, such a measurement is difficult, as the shape and structure of the pulsar beam is unknown but often needed in modeling geodetic precession. In fact, spin precession is often used (as the only way!) to *infer* 2-D beam information (see Section 4.3. This is different when polarisation measurements reveal the (changing) geometry. Indeed, the first quantitative measurement of relativistic spin-precession in binary pulsars was possible with polarisation measurements of PSR B1534+12 (see Section 3.2) albeit with limited precision. A much better test was enabled with the spin precession seen via the eclipses in the Double Pulsar (see Section 3.5 where a 13% precision was achieved in a strong-field regime. Due to our ability to independently measure both orbits in the system, we can use the result also to put first constraints on alternative theories of gravity.

After the introducing of the method by Breton et al. (Ref. 45), Kramer & Wex (Ref. 15) describe in detail how the relativistic spin-precession rate of pulsar B (see Section 3.5), can be interpreted in formalism introduced by Will⁴⁶ and Damour and Taylor.¹⁹ These authors constructed a Lagrangian that generalizes the Lagrangian of the post-Newtonian orbital dynamics in a strong-field regime, for fully conservative theories of gravity (modified Einstein-Infeld-Hoffmann formalism). In particular, to account for strong-field effects in the spinorbit interaction, Damour & Taylor introduced the coupling function Γ_i^j in the spin-orbit Lagrangian of Ref. 47, where the indices i and j refer to the two bodies in the system. The measured relativistic

spin-precession rate of pulsar B can now be used to limit, for the first time, Γ_B^A as

$$\Omega_{p,B} = n_b X_A X_B \left[(1+R) \frac{\Gamma_B^A}{\mathcal{G}} - \frac{R}{2} \right] \frac{\beta_O^2}{1-e^2}, \quad (3)$$

where $\beta_O \equiv (\mathcal{G} M n_b)^{1/3}/c$ is a characteristic velocity for the relative orbital motion and $n_b = 2\pi/P_b$ is the orbital frequency. In general relativity $\mathcal{G} = G$, but in alternative theories of gravity the actual value depends on the parameters of the theory and of the structure of each body. In other words, for neutron stars these parameters can deviate significantly from their values in general relativity, even if their weak-field limit agrees with general relativity.^{46,48} The fact that the Double Pulsar gives access to the mass ratio,

$$R \equiv \frac{m_A}{m_B} = \frac{a_B}{a_A} = \frac{a_B \sin i/c}{a_A \sin i/c} \equiv \frac{x_B}{x_A}. \quad (4)$$

in any Lorentz-invariant theory of gravity,^{39,49} allows us to determine $X_A = R/(1+R) = 0.51724 \pm 0.00026$ and $X_B = 1/(1+R) = 0.48276 \pm 0.00026$. As detailed in Ref. 15, with this information the measurement of the shape of the Shapiro delay, s , can be used to determine β_O via

$$s = \frac{n_b x_A}{\beta_O X_B}, \quad (5)$$

to $\beta_O = (2.0854 \pm 0.0014) \times 10^{-3}$. Consequently

$$\frac{\Gamma_B^A}{2\mathcal{G}} = 0.95 \pm 0.11, \quad (6)$$

As pointed out in Ref. 15, this is not only in agreement with general relativity, which predicts $\Gamma_B^A/2\mathcal{G} = 1$, but it also demonstrates that the relativistic precession of a spinning body is independent of its internal structure. They emphasise that currently the Double Pulsar is the only system that allows for the test of the “effacement” property of a spinning body.

4.2. Core collapse physics & neutron star birth

As described in Section 2.1.3, the evolutionary history of most binary pulsars involves a phase of mass transfer after which we would usually expect the spin vectors of the stars to be aligned with the orbital momentum vector. If a supernova (SN) occurs after this alignment, a kick may be imparted on the newly born neutron star, tilting the post-SN orbit relative to the pre-SN configuration. Modeling the observed effects of relativistic spin precession, we can determine the misalignment angle between the spin vector of the precessing neutron star (see Ref. 26 and Sections above). This information can be used to infer the pre-SN configuration which can then be compared to the observed post-SN situation in order to learn about the SN explosion itself, such as the kick amplitude and direction.

Such an application of spin precession was first achieved by Wex et al. (Ref. 50) who used the geometry of the PSR B1913+16 system²⁶ to derive that the kick

was relatively large and its direction rather well confined. This type of analysis involves tracing the motion of the binary back in time to potential birthplaces in the plane of the galaxy, assuming that the large binary mass remaining after the first SN meant that the space velocity at that time would not be large. The gravitational radiation decay of the orbital eccentricity and separation must also be corrected for.⁵¹ The kick magnitude and progenitor mass can then be constrained using simple equations.⁵² To achieve the result, one also has to make assumptions about the possible characteristics of the exploding He-star. The latter input and the applied techniques were subsequently refined and applied by Kalogera and her group (e.g. Refs. 53,54) who performed similar work for instance for PSR B1534+12 and the Double Pulsar. Their results can be compared with work by other authors, who all agree that spin precession results for PSR B1534+12 suggest that its companion received a large kick with velocities of $200 - 270 \text{ km s}^{-1}$ and progenitor masses were of $2.00 - 3.35 M_{\odot}$.^{53,55} For the Double Pulsar the results of similar calculations differ, partly because of the role of the unknown radial velocity of the system, but also because the system has a number of peculiar properties.

On one hand, the mass of pulsar B is small, only $1.25 M_{\odot}$,³ prompting the argument that B might not have formed in an iron core collapse but may have been born in an electron-capture supernova, in which a slightly less massive O-Ne-Mg core captures electrons onto Mg to initiate the collapse.⁵⁶ On the other hand, the derived very small systemic velocity of the Double Pulsar (corrected for Galactic rotation) of only $9_{-3}^{+6} \text{ km s}^{-1}$ (see Refs. 3,57) indicates that, depending on the progenitor mass of B, the kick velocity was small (e.g. Refs. 58–61) but see the review by Kramer & Stairs (Ref. 62) for a detailed discussion of the various results. What seems to be clear from the absence of any profile changes in pulsar A, is that the misalignment vector in A must be rather small, consistent with a “gentle”, low-velocity kick birth of young pulsar B (e.g. Ref. 61).

Finally, a similar study based on the geometry derived from spin precession for PSR J1141–6545 suggests that the pre-supernova star had a mass of only $\sim 2 M_{\odot}$ and that the supernova kick velocity was relatively small, between 100 and 250 km s^{-1} depending on the assumed systemic velocity.²⁵

4.3. Pulsar Beam Tomography

As our changing line-of-sight intersects the pulsar emission beam, relativistic spin precession provides the only way to actually map the structure of the radio beam. This idea^{16,23} of a “beam tomography” was first beautifully applied to PSR B1913+16^{27,28,63} where it was shown that the simple hollow cone structure (filled with a core component) is perhaps oversimplified but not too far from the truth. Deviations from a purely circular beam are observed, suggesting an elongation of the beam in North-South direction. The initially suggested hourglass shape of the emission beam^{27,28} appears to be too extreme given the new improved modeling.⁶³

It is interesting to see whether the emission beams of recycled pulsars look

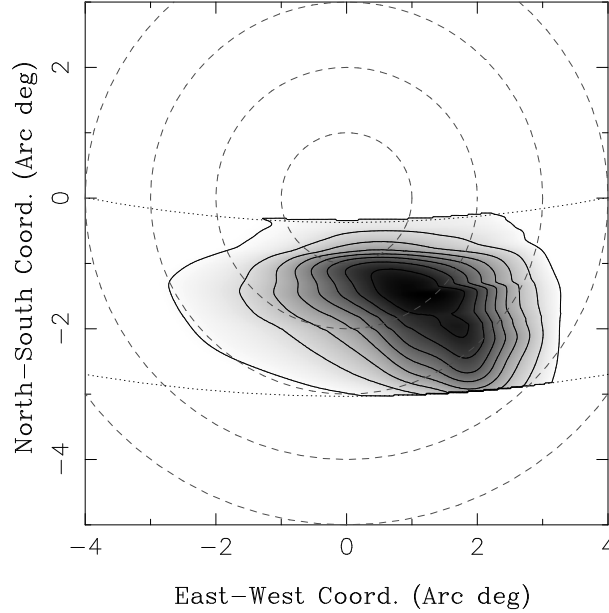


Fig. 6. Beam map derived for PSR J1141–6545 in Ref. 25.

different from those of young pulsars. The first non-recycled pulsars for which we can infer the beam pattern is PSR J1141–6545 where the geometry suggests that we only see one half of the polar-cap region. Despite this we can clearly see that the beam is quite asymmetric with no evidence for a core-cone or ring structure that is symmetric about the magnetic pole. The partially filled beam can be described as “patchy”, albeit with just one major patch in the region scanned so far. This is the first two-dimensional map of an emission beam to clearly show such patchy structure (Fig. 6). Even though the observed pulse *width* is about average, the inferred beam *radius* is rather small, given that the so far observed emitting region fits within a circle of radius about 4 deg centered on the magnetic axis. This is much smaller than the ~ 10 deg expected from the period scaling derived from other pulsars (e.g. Refs.^{64–66}). Time will tell – by transversing more of the pulsar beam – whether the beam really happens to be smaller than usual or whether a large elongation of the pulsar beam is present.

We already indicated that beam tomography can also be performed for pulsar B in the Double Pulsar system. Here, the results show that the observed beam structure cannot be easily explained with a circular hollow-cone beam either, but that the beam appears to be elliptical and horse-shoe shaped. This unusual shape may find its origin in the strong interaction of the pulsar wind of A with the magnetosphere of B, which distorts B’s magnetosphere and produces a cometary shape. As a result, B was only strongly detectable in two specific orbital phase ranges.³⁹ We can therefore expect the magnetospheric currents to be significantly different from

“normal”, undisturbed magnetospheres, so that the result is extremely interesting in order to learn more about the exotic conditions in this system, but it is less likely that the derived beam tomography gives a representative example for the whole pulsar population.

5. Summary & Conclusions

From the humble beginnings of detecting profile changes in the Hulse-Taylor pulsar as the first observational evidence for relativistic spin precession in binary pulsars, the study of the associated effects has become routine. Indeed, it is fair to say that relativistic spin precession has been established as a tool for the study of physical and astrophysical problems. Today, studies of spin precession have led to the first and only constraints for spin-orbit coupling of strongly self-gravitating bodies, it has been used to reveal the previously unknown structure of pulsar emission beams and it has been instrumental in providing evidence that the magnitude of kicks imparted on neutron stars during their birth can cover a wide range of magnitude, essentially from 10 to 1000 km s⁻¹. In the years to come, further studies will reveal new results and we indeed look forward to the observations of spin precession in the first pulsar - black hole system, the discovery of which we await so eagerly.

Acknowledgments

I am grateful to the conference organisers for their hospitality and a memorable event.

References

1. C. Will, *Living Reviews in Relativity* **9**, 1 (2006), URL (Cited on 2010/06/16): <http://relativity.livingreviews.org/Articles/lrr-2006-3>.
2. I. I. Shapiro, *Phys. Rev. Lett.* **13**, p. 789 (1964).
3. M. Kramer, I. H. Stairs, R. N. Manchester, M. A. McLaughlin, A. G. Lyne, R. D. Ferdman, M. Burgay, D. R. Lorimer, A. Possenti, N. D’Amico, J. M. Sarkissian, G. B. Hobbs, J. E. Reynolds, P. C. C. Freire and F. Camilo, *Science* **314**, 97 (2006)).
4. W. de Sitter, *MNRAS* **77**, p. 155 (1916).
5. A. D. Fokker, *Koninklijke Nederlandse Akademie van Wetenschappen Proceedings Series B Physical Sciences* **23**, 729 (1921).
6. G. Boerner, J. Ehlers and E. Rudolph, *A&A* **44**, 417 (1975).
7. D. R. Lorimer and M. Kramer, *Handbook of Pulsar Astronomy* (Cambridge University Press, 2005).
8. M. M. Komesaroff, *Nature* **225**, 612 (1970).
9. J. M. Rankin, *ApJ* **352**, 247 (1990).
10. J. M. Rankin, *ApJ* **405**, 285 (1993).
11. A. G. Lyne and R. N. Manchester, *MNRAS* **234**, 477 (1988).
12. M. Kramer and S. Johnston, *MNRAS* **390**, 87 (2008).
13. V. Radhakrishnan and D. J. Cooke, *Astrophys. Lett.* **3**, 225 (1969).
14. K. M. Xilouris, M. Kramer, A. Jessner, A. von Hoensbroech, D. Lorimer, et al., *ApJ* **501**, 286 (1998).

15. M. Kramer and N. Wex, *Classical and Quantum Gravity* **26**, 073001 (2009).
16. T. Damour and R. Ruffini, *Academie des Sciences Paris Comptes Rendus Ser. Scie. Math.* **279**, 971 (1974).
17. R. A. Hulse and J. H. Taylor, *ApJ* **195**, L51 (1975).
18. B. M. Barker and R. F. O'Connell, *Phys. Rev. D* **12**, 329 (1975).
19. T. Damour and J. H. Taylor, *Phys. Rev. D* **45**, 1840 (1992).
20. J. Antoniadis, C. Bassa, N. Wex, M. Kramer and R. Napiwotzki, *A&A* submitted (2010).
21. A. J. Faulkner, I. H. Stairs, M. Kramer, A. G. Lyne, G. Hobbs, et al., *MNRAS* **355**, 147 (2004).
22. I. H. Stairs, S. E. Thorsett and Z. Arzoumanian, *Phys. Rev. Lett.* **93**, p. 141101 (September 2004).
23. J. M. Weisberg, R. W. Romani and J. H. Taylor, *ApJ* **347**, 1030 (1989).
24. J. M. Cordes, I. Wasserman and M. Blaskiewicz, *ApJ* **349**, 546 (1990).
25. R. N. Manchester, M. Kramer, I. H. Stairs, M. Burgay, F. Camilo, et al., *ApJ* **710**, 1694 (2010).
26. M. Kramer, *ApJ* **509**, 856 (1998).
27. J. M. Weisberg and J. H. Taylor, General relativistic precession of the spin axis of binary pulsar B1913+16: First two dimensional maps of the emission beam, in *Pulsar Astronomy - 2000 and Beyond, IAU Colloquium 177* M. Kramer, N. Wex and R. Wielebinski (eds.), (Astronomical Society of the Pacific, San Francisco, 2000), pp. 127–130.
28. J. M. Weisberg and J. H. Taylor, *ApJ* **576**, 942 (2002).
29. Z. Arzoumanian, PhD thesis, Princeton University 1995.
30. I. H. Stairs, S. E. Thorsett, J. H. Taylor and Z. Arzoumanian, Geodetic precession in PSR B1534+12, in *Pulsar Astronomy - 2000 and Beyond, IAU Colloquium 177* M. Kramer, N. Wex and R. Wielebinski (eds.), (Astronomical Society of the Pacific, San Francisco, 2000), pp. 121–124.
31. V. M. Kaspi, A. G. Lyne, R. N. Manchester, F. Crawford, F. Camilo, et al., *ApJ* **543**, 321 (2000).
32. A. W. Hotan, M. Bailes and S. M. Ord, *ApJ* **624**, 906 (2005).
33. R. N. Manchester, A. G. Lyne, N. D'Amico, M. Bailes, S. Johnston, et al., *MNRAS* **279**, 1235 (1996).
34. D. R. Lorimer, I. H. Stairs, P. C. Freire, J. M. Cordes, F. Camilo, et al., *ApJ* **640**, 428 (2006).
35. L. Kasian, et al., Timing and Precession of the Young, Relativistic Binary Pulsar PSR J1906+0746, in *40 Years of Pulsars: Millisecond Pulsars, Magnetars and More*, ed. C. Bassa, Z. Wang, A. Cumming, & V. M. Kaspi, American Institute of Physics Conference Series, Vol. 983 (2008).
36. G. Desvignes, I. Cognard, M. Kramer, A. Lyne, B. Stappers and G. Theureau, Change in the pulse component separation for PSR J1906+0746, in *40 Years of Pulsars: Millisecond Pulsars, Magnetars and More*, ed. C. Bassa, Z. Wang, A. Cumming, & V. M. Kaspi, American Institute of Physics Conference Series, Vol. 983 (2008).
37. G. Desvignes, PhD thesis, Orleans University (2010).
38. M. Burgay, N. D'Amico, A. Possenti, R. N. Manchester, A. G. Lyne, et al., *Nature* **426**, 531 (2003).
39. A. G. Lyne, M. Burgay, M. Kramer, A. Possenti, R. N. Manchester, et al., *Science* **303**, 1153 (2004).
40. R. N. Manchester, M. Kramer, A. Possenti, A. G. Lyne, M. Burgay, et al., *ApJ* **621**, L49 (2005).

41. R. D. Ferdman, I. H. Stairs, M. Kramer, R. N. Manchester, A. G. Lyne, et al., The double pulsar: evolutionary constraints from the system geometry, in *40 Years of Pulsars: Millisecond Pulsars, Magnetars and More*, ed. C. Bassa, Z. Wang, A. Cumming, & V. M. Kaspi, American Institute of Physics Conference Series, Vol. 983 (2008).
42. R. D. Ferdman, PhD thesis, University of British Columbia (2008).
43. M. Burgay, A. Possenti, R. N. Manchester, M. Kramer, M. A. McLaughlin, et al., *ApJ* **624**, L113 (2005).
44. B. Perera, M. McLaughlin, M. Kramer, I. Stairs, R. Ferdman, et al., *ApJ* in press (2010).
45. R. P. Breton, V. M. Kaspi, M. Kramer, M. A. McLaughlin, M. Lyutikov, et al., *Science* **321**, 104 (2008).
46. C. M. Will, *Theory and Experiment in Gravitational Physics* (Cambridge University Press, Cambridge, 1993).
47. T. Damour, *Academie des Sciences Paris Comptes Rendus Ser. Scie. Math.* **294**, p. 1355 (1982).
48. T. Damour and G. Esposito-Farese, *Phys. Rev. D* **54**, 1474 (1996).
49. T. Damour, *arXiv:0704.0749*, (2007).
50. N. Wex, V. Kalogera and M. Kramer, *ApJ* **528**, 401 (2000).
51. P. C. Peters, *Phys. Rev.* **136**, 1224 (1964).
52. V. Kalogera, *ApJ* **471**, 352 (1996).
53. B. Willems, V. Kalogera and M. Henninger, The formation of the most relativistic pulsar psr j0737-3039, in *Binary Radio Pulsars*, eds. F. Rasio and I. H. Stairs (Astronomical Society of the Pacific, San Francisco, 2005).
54. V. Kalogera, F. Valsecchi and B. Willems, Neutron Stars: Formed, Spun and Kicked, in *40 Years of Pulsars: Millisecond Pulsars, Magnetars and More*, ed. C. Bassa, Z. Wang, A. Cumming, & V. M. Kaspi, American Institute of Physics Conference Series, Vol. 983 (2008).
55. S. E. Thorsett, R. J. Dewey and I. H. Stairs, *ApJ* **619**, 1036 (2005).
56. P. Podsiadlowski, J. D. M. Dewi, P. Lesaffre, J. C. Miller, W. G. Newton and J. R. Stone, *MNRAS* **361**, 1243 (2005).
57. A. T. Deller, M. Bailes and S. J. Tingay, *Science* **323**, 1327 (2009).
58. T. Piran and N. J. Shaviv, *Phys. Rev. Lett.* **94**, p. 051102 (2005).
59. T. Piran and N. J. Shaviv, *astro-ph/0603649* (2006).
60. B. Willems, J. Kaplan, T. Fragos, V. Kalogera and K. Belczynski, *Phys. Rev. D* **74**, p. 043003 (2006).
61. I. H. Stairs, S. E. Thorsett, R. J. Dewey, M. Kramer and C. A. McPhee, *MNRAS* **373**, L50 (2006).
62. M. Kramer and I. H. Stairs, *Ann. Rev. Astr. Ap.* **46**, 541 (2008).
63. T. Clifton and J. M. Weisberg, *ApJ* **679**, 687 (2008).
64. J. A. Gil, J. Kijak and J. H. Seiradakis, *A&A* **272**, 268 (1993).
65. D. M. Gould, PhD thesis, The University of Manchester (1994).
66. M. Kramer, R. Wielebinski, A. Jessner, J. A. Gil and J. H. Seiradakis, *A&AS* **107**, 515 (1994).